Asian J. Exp. Sci., Vol. 32, No. 2, 2018; 1-14

Online available on : www.ajesjournal.com, ISSSN : 0971-5444

Petrology of Volcanic and Pyroclastic Rocks in Northwest Hassan Abad (Northeast Esfahan)

Mozhgan Poormansouri[1], Mohammad Hossein Razavi[1]*, Afshin Ashja Ardalan[1], Mohammad Ali Makkizadeh[2], Mohammad Khalaj[3]

[1]Geology Department, Tehran North Branch, Islamic Azad University, Tehran, Iran
[2]Geology Department, University of Esfahan, Esfahan, Iran
[3]Geology Department, Payam-e Noor University of Tehran, Tehran, Iran
Corresponding author : * razavi.khu@gmail.com
Received: December 28, 2017; Revised: March 15, 2018; Accepted: March 22, 2018

Abstract : Hassan Abad Region is located 180 kilomteres to the northeast of Esfahan along Uremia – Dokhtar Magmatic Belt. Most outcrops in this region belong to Eocene volcanic activity with rhyolite and tuff composition. The rhyolites consist of quartz, plagioclase, alkali feldspar minerals and glass fragments. The tuffs are of crystaline, vitric and ignimbrite typecropping out as interconnected domes along the great fault of Qom – Zofreh with a northern – southern trend. According to geochemical studies and diagrams, the constituent magma of the respective rocks with rholitic composition is classified in calc-alkaline series, and based on spider diagrams of the samples in the studied area, originates from partial melting of custral rocks. Discordant trends of Uremia – Dokhtar Belt and reverse faults as well as regional dykes according to Rieldel model imply that most volcanic and volcanoclastic rocks are subject to simple shear stress in the shear – compressional system (Bargowhar and Marbin – Rangan faults and Kachumesghal – Ganyan fault).

Keywords: Petrology, Hassan Abad, Uremia – Dokhtar Belt, Rhyiolite, Pyroclastic.

Introduction

Hassan Abad Region is situated 180 kilometers to the northeast of Esfahan and 40 kilometers to the southwest of Adrestan in Central Iran stuctural zone, Uremia– Dokhtar magmatic arc and along Qom– Zofreh fault system. This region represents a volcanic– sedimentary setting. The studied volcanic rocks are part of the techno-magmatic unit, which has been formed as a thick extensive series of volcanic and dependent pyroclastic rocks. (Fisher, 1966: Fisher & Schmineke, 1984). Therefore, taking into account the fact the pyroclastic masses have not been comprehensively studied up to now and no codified information are available about their petrogenesis, it is attempted in the present research to study the petrography and petrogenesis of volcanic and pyroclastic masses via benefitting from the latest acquired sicentific achievements.

2. Research Methodology

At first review of literature was made and the geological maps of Hassan Abad Region and surrounding areas were consulted. The area was studied in field. Locations of samples were determined using GPS at different time intervals. Images were recorded from notable outcrops and contacts. Seventy thin sections of rocks were studied in laboratory under polarized microscope in order to determine the mineralogical and petrological of the rocks along with micro-textures. Further, for nomenclature of the studied rocks, ICP-MS and SDF techniques were applied to measure the contents of principle elements, rare elements, and rare-earth elements (REEs) of the samples. In the final stage of the research also, the data obtained from field survey, petrographic studies, and laboratory measurements were integrated and analyzed.

3 – Geology and Tectonics of the Region:

Hassan Abad Region is located between geographical coordinates of northern latitudes of 33° 07` and 33° 26` and eastern longitudes of 51° 56`and 52° 27` in the central part of Uremia– Dokhtar strip (Fig. 1). Based on field studies, the rock units in this region are in the form of a volcanic– sedimentary series belonging to Eocene to Oligocene epochs. It seems that major activity in the respective region have started from Mid-Eocene, and as a result, these rocks are product of volcanic activities during Middle – Late Eocene. Ryholite units are older than andesite and trachybasalt– trachyandesite units, and, the ignimbrite and trachyte units are the youngest units. The mentioned activities have mainly occurred in continental or shallow and coastal environments (Emami, 2000). In this region, most outcrops are associated with Eocene volcanic activity with rhyolite, andesite, and dacite lithologies in which ignimbrite tuffs are observed as well (Fig. 2 A & B).

Fig. 1 – Access ways to the region of study

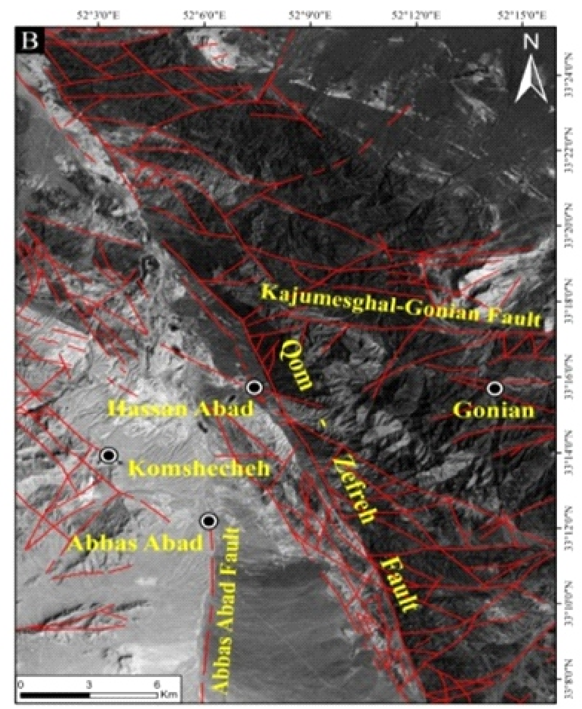

Fig. 2 - (B) Determination of major faults of the region on LANDSAT image using band ratio of RGB: 743

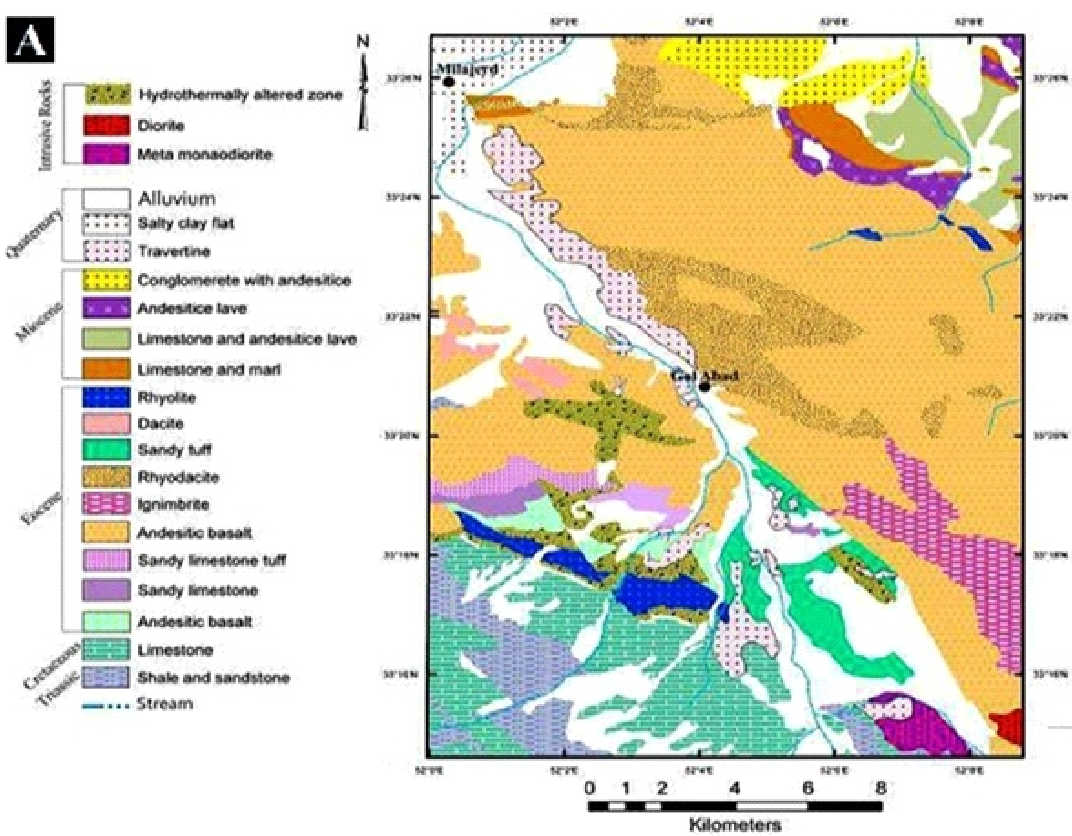

Fig. 2- (A) Geological map of the studied region, derived from 1:100,000 geological map of Ardestan (Emami & Hourdfar, 2010)

In the studied region, reserve faults of Bargowhar, Marbin - Rangan, and Kachumesghal – Ganyan fault are situated in the northeast of Qom – Zofreh fault. Bargowhar and Marbin – Rangan fault dips to southwest and dip direction of Kachumesghal – Ganyan fault is toward northeast. Shear and compressional components resulting from movement of the respective faults have caused strike-slip displacements along Qom – Zofreh fault and folding and reverse faulting over the trends with the same strike (Pourmansouri, 2015). Tuffs which are locally ignimbrite in certain points have exposures as relatively elevated domes and hills along northern – southern direction and aligned with the strike of the regional faults. Intense alteration is observed along Kachumesghal – Ganyan fault zone. Volcanic deposits aging Middle Eocene in the northern part contact with the fault block (Fig. 12).

Strike-slip regimes were created by three mechanisms namely pure shear, simple shear, and combination of pure and simple shears. Pure shear deformation causes conjugate strike-slip faults, folding, and normal faults (Fig. 3). In this type of deformation, the strike-slip faults form a 30-degree angle with the direction of the largest principle axis of stress. This model is commonly known as Columb – Anderson's model (Sylvester 1988). Based on the conducted analyses, it was revealed that the regional faults have been formed due to performance of simple shear exerted on Uremia – Dokhtar belt. Changes have occured in the fault trends with continuation of shear regime and progressive deforation in the faults and the geomtrical relations between them. Therefore, due to discordant trends of Uremia – Dokhtar Belt and the reverse faults and regional dykes, Riedel model suggest that most volcanic masses of the region have been implaced under simple shear in the shear and compressional system (Bargowhar and Marbin – Rangan faults and Kachumesghal – Ganyan fault).

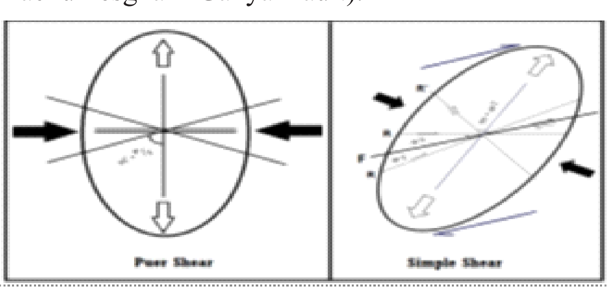

Fig. 3 – Comparison between simple shear and pure shear mechanisms; figures on the left and right sides respectively represent Columb-Andreson and Riedel models

4- Petrography

Field surveys and petrography indicate that the rock units in the region exhibit a low lithological diversity and have mainly acidic composition. The predominant lithology is rhyolite and pyroclastic rocks, and, the pyroclastic rocks include lithic tuff, crystalline vitric tuff, crystalline vitric lithic tuff, vitric tuff, and ignimbrite (Fisher, 1966).

4 – 1 – Rhyolite:

Rhyolites are observed as small hills along with dependent tuffs. Their color is mostly pea yellow to pink and mainly extremely light grey. Rhyolites are fine-grained and mainly contain vitric fragments and pores suggesting their rapid cooling at ground surface. In Hassan Abad Region, highly viscous rhyolites have outcrop in the studied region in the form of dome along Qom– Zofreh stike-slipe fault (Fig. 5) and are situated in contact with metamorphosed and altered sedimentary rocks of Jurassic age. Volcanic rocks of Hassan Abad Region consist of rhyolite and tuff outcrops with the age attributed to Eocene. This region is located in the middle part of Uremia – Dokhtar strip and is classified in rhyolite group in terms of mineralogy and chemical composition. This felsic volcanic mass has a porphyry felsic and spherolitic texture containing quartz, plagioclase, alkali feldspar, and opaque minerals (Fig.4-A&B). From mineralogical standpoint, rhyolites contain fragmented quartz crystals as well as alkali feldspars distributed over a matrix of the same fragmented crystals and glaass (Fig. 5-A).

Despite the fact that plagioclase and quartz crystals were completely crushed from the sides, atoll textures are also observed in a limited number of them. In addition, rounded margin and reabsorption is also seen here and there in the alkali feldspars. Furthermore, cryptocrystaline texture can be also considered for this rock because consolidated ash seems to be present in their matrices because glass-like isotope is clearly detected under cross-polarized light (XPL). Latent crystal matrix has been somewhat recrystalized in certain points such that fine-grained crystals of felsic (quartz and feldspar) have dominated the matrix (Fig. 5-B & C). It is noteworthy that sphereolitic texture is also seen in certain points of matrix to a limited extent (Fig. 6-A). This texture results from semi-radial recrystallization of glass. A shadow of semi-radial forms of quartz feldspar crystals can be observed on the phenocryst plagioclase (acting as the nucleus). In scarce instances, complete substitution of initial mafic phenocryst of the rock (probably biotite or amphibole) by mucovite) is detected (pseudomorphism) which is possibly caused by alteration and potassic metasomatism (Fig. 7).

Fig. 4 – A, B: view of dome-shaped rhyolites in Hassan Abad Region

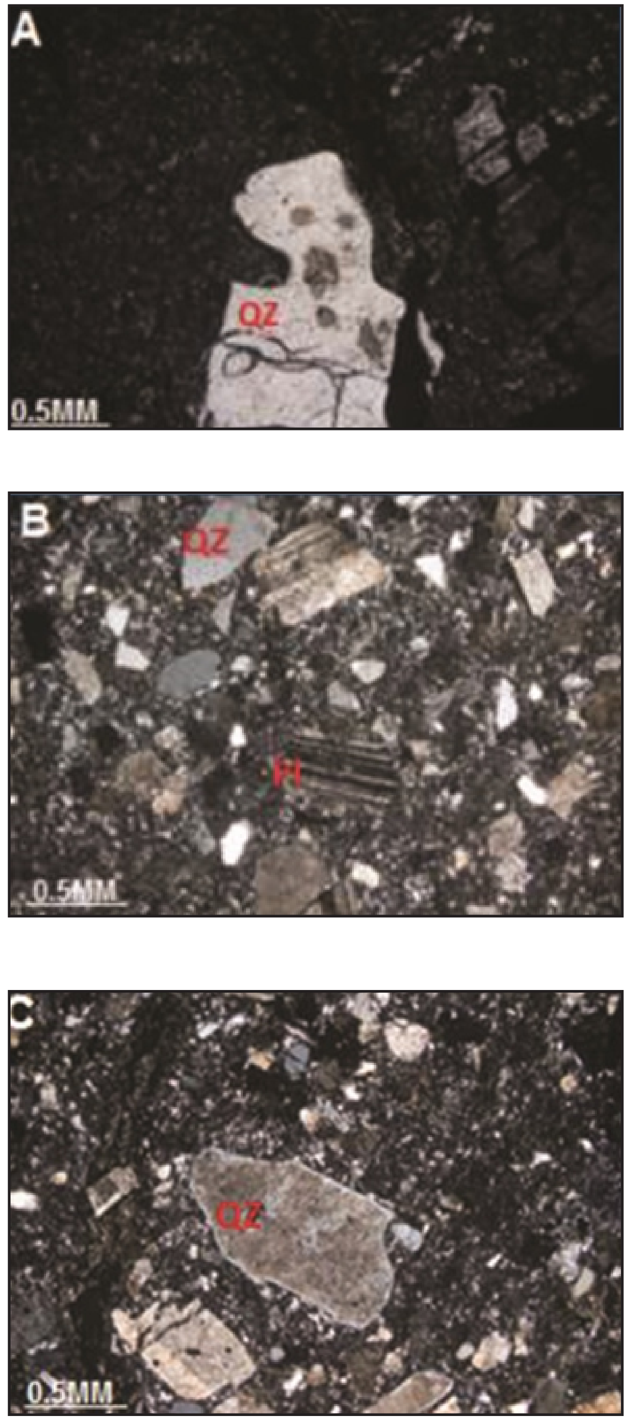

Fig. 5 – A: Quartz crysrals are completely broken from the sides; B: Broken quartz and alkali feldspar crystals over a matrix of the same crystal fragments and glasses; C: rounded margin and reabsorption of alkali feldspars (P1 = plagioclase mineral; Qz = quartz mineral) (XPL)

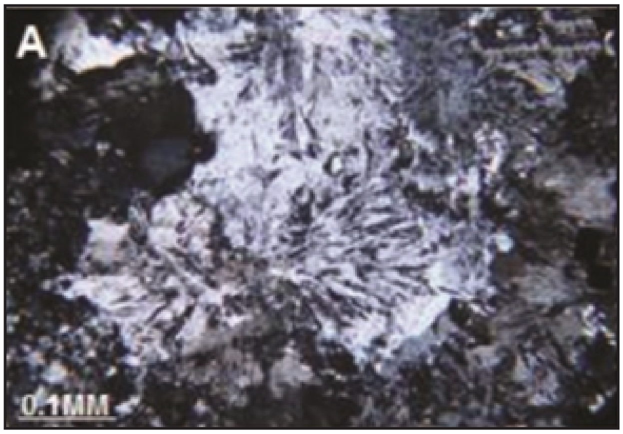

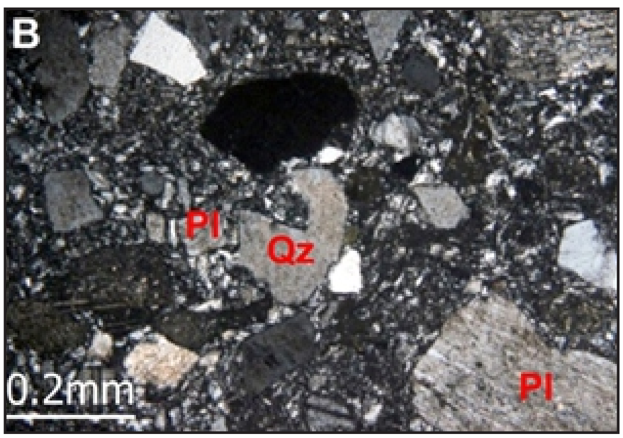

Fig. 6 – A - Sphereolitic texture in rhyolite (XPL 100), B – Microscopic section of rhyolite, quartz with embayment over a matrix of alkali feldspar and plagioclase and galls within a fine-grained texture (PPLx40)

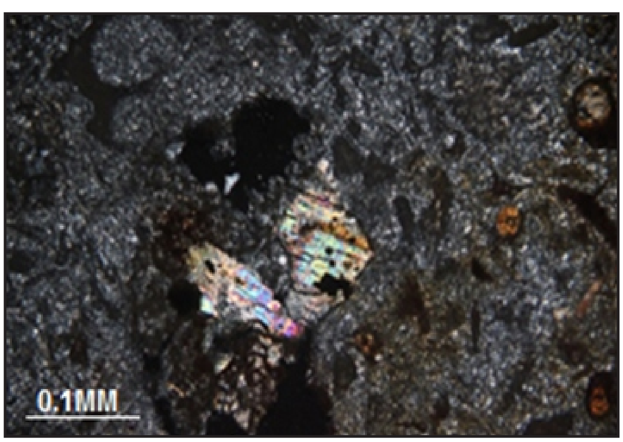

Fig. 7 - Complete substitution of initial mafic phenocryst of the rock (probably biotite or amphibole)by muscovite can be observed (Ms: muscovite mineral) (XPL×100)

4 – 2 –Tuff

Tuff refers to pyroclastic rocks in which over 75% of the fragments were smaller than 2 (mm). Based on size of fragments, tuffs were divided into coarse-grained and fine-grained categories. They were also classified into vitric tuff, crystalline tuff, and lithic tuff depending on the type of fragments. The color of this rock is frequently (not entirely) green in the manual samples of the studied region. The samples were classified in rhyolite interval following analysis and plotting of geochemical diagrams.

Based on petrographic evidences, the studied tuffs were categorized as crystal-vitric tuffs due to possession of lithic, glass, and crystal fragments. Numerous minerals including quartz and plagioclase were formed in this type of tuffs. Quartz phenocrysts occasionally have embayment in the margins. Plagioclase phenocrysts have regular or irregular albite twins and are eroded and angular from the edges (Fig. 5-B). This mineral is severely decomposed, and because of saussuritization, is transformed into a series of epidote, chlorite and calcite minerals (Fig. 9-B).

Lithic Tuff

Lithic tuff constitutes part of the region's tuffs in which lithic fragments are abundantly found. Lithic fragments were observed at various sizes from 0.1 to 0.5 cm in the rocks. The respective fragments were mainly rounded and composed of plagioclase (phenocryst and microphenocryst) and alkali feldspar (Fig. 8).

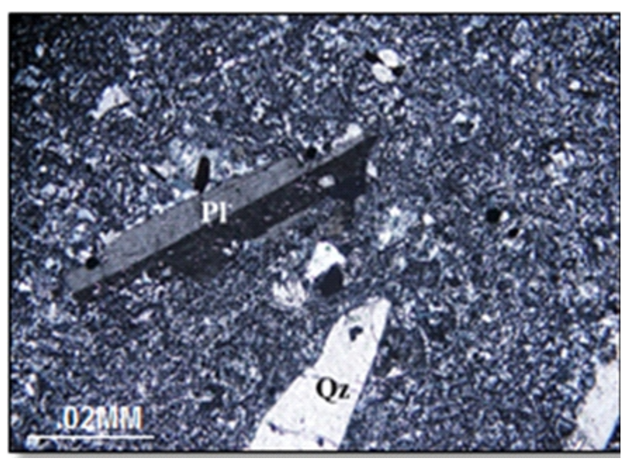

Fig. 8 – A view of lithic tuff, plagioclase and quartz crystals in fine-grained matrix (XPL×40)

Crystal-vitric Tuffs

Crystal-vitric tuffs of the region consist of mineral pieces and vitric fragments. In this set of tuffs, numerous mineral were observed as below:

Quartz: this mineral is detectable in rock as phenocryst with occasional embayment in the margins.

Plagioclase: Plagioclase phenocrysts have regular and irregular albite twins and are eroded to angular from the edges (Fig. 9-A). This mineral is intensely decomposed and altered into sericitic and calcite minerals and so on (Fig. B-9).

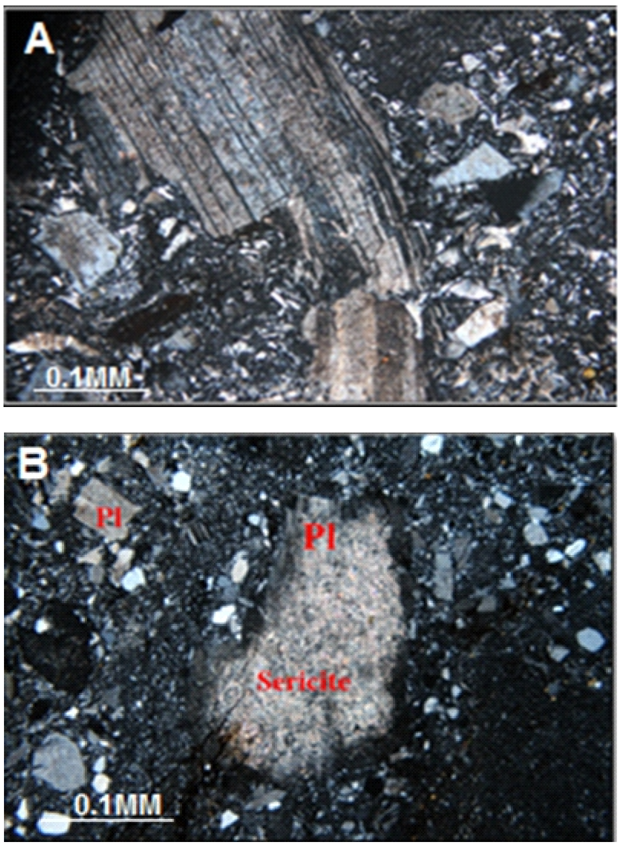

Fig. 9-A: Plagioclase phenocryst with polysynthetic twin (XPL×100); a weak bending caused by tectonic activity is observed in twin surfaces B –Effects of sauricitization decomposition in plagioclase phenocryst (XPL×100)

Pyroxene: This mineral was observed in small amount and as phenocryst, mainly decomposed into chlorite.

Sericite: Having a relative weak relief, this mineral has mainly replaced feldspar in the rock (Figure 10).

Opaque minerals: Glass fragments were replaced by iron oxide and can be sparsely observed

Apatite: This mineral is seen as bar-shaped inclusions in quartz phenocrysts.

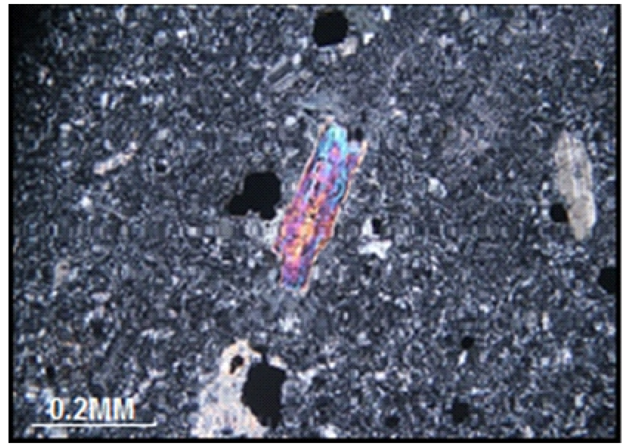

Fig. 10 –Complete substitution of fine-grained muscovite with sericite in feldspar framework (XPL×40)

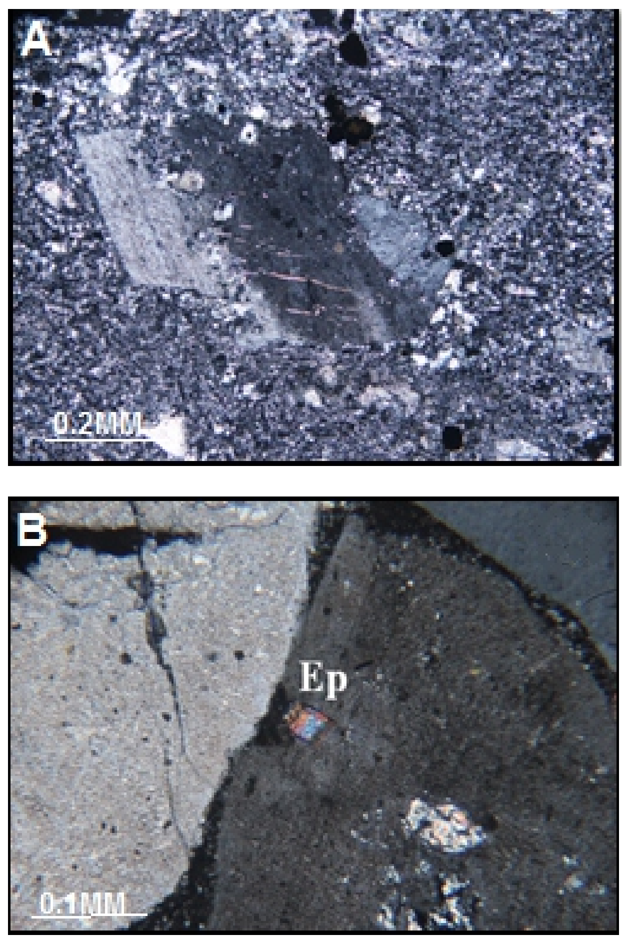

Fig. 11-A: Presence of feldspar phenocryst in fine-grained felsic matrix of the rock (XPL×40) B- Presence of epidote within the minerals (XPL×100)

Pyrite: This mineral is replaced by iron oxide and is pseudomorph. Apatite and zircon mineral (secondary) are also present where apatite is seen as inclusion in feldspar and the feldspars are carbonated in some parts as well.

Epidote: This mineral has strong relief, green color and is formed in interstitial or fissure filler form, and, as a result of decomposition of calcium-bearing minerals like pyroxene and plagioclase.

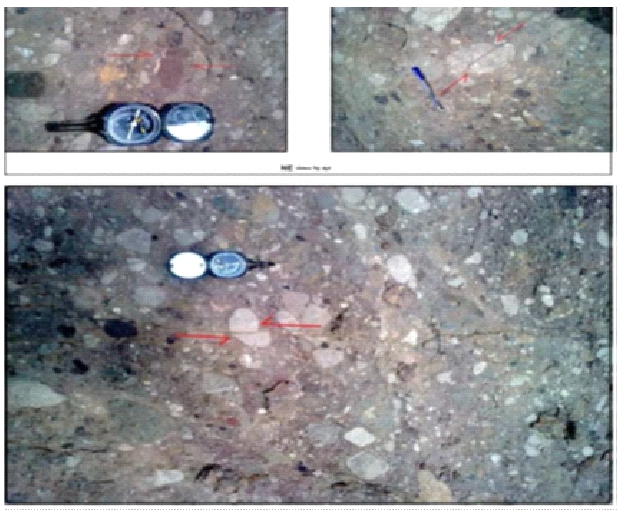

Fig. 12 – Alteration in Eocene volcanic deposits created by sinisteral strike-slip displacement of Kachumesghal – Ganyan Fault (Mahjal, 2000)

Vitric Tuff:

Vitric tuff samples were mainly composed of vitric fragments (glass shards) together with little amount of crushed crystals.

Glass shards were observed with different shapes and sizes and in light brown color, low relief under normal light and dark interference color under polarized light. These shards exhibit flowing state and were of chevron type (Fig. 13).

Quartz:

This mineral in these rocks appear as large, amorphous, and crushed phenocrysts and have edges with embayment and amoeba-like and rounded boundaries.

Plagioclase: This mineral was seen as megacryst, phenocryst, and microlite in the rock. Some of the minerals have compound albite– carlsbad twin and most of them are crushed from the edges forming angular and/or rounded margins.

Sericite: This one was among the secondary minerals and can be found in the rocks.

Pyrite: This mineral appears as pseudomorph and remnants of elongated and decomposed ferromagnesian minerals (Mg, Fe).

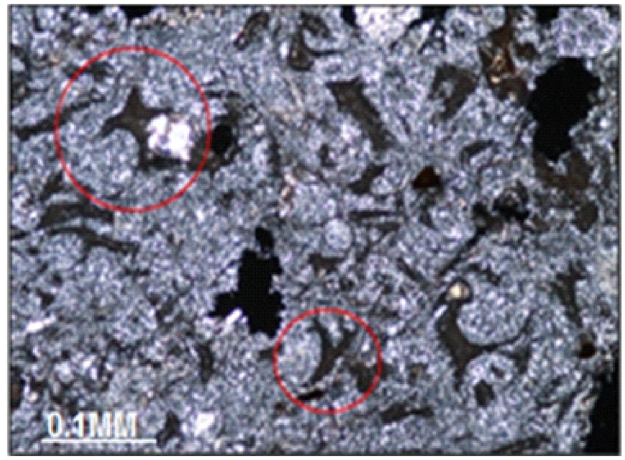

Fig. 13 – Representation of y-shaped chevron shards (XPL×100)

4 – 3 – Ignimbrite:

Petrographic observations indicate that elongation with flow of glass fragments (Fiame) were occasionally observed in some smaples reflecting presence of ignimbrite or welded tuff. Welded tuffs are stacked hot ashes. Weight of upper layers has caused welding and widening of glasses at high temperatures (Fig. 14-A & B).

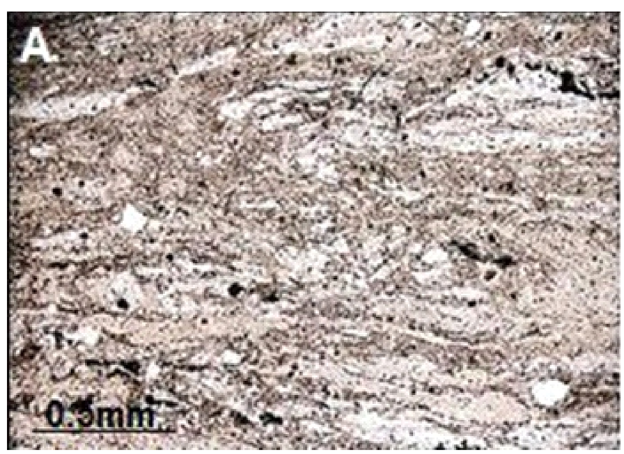

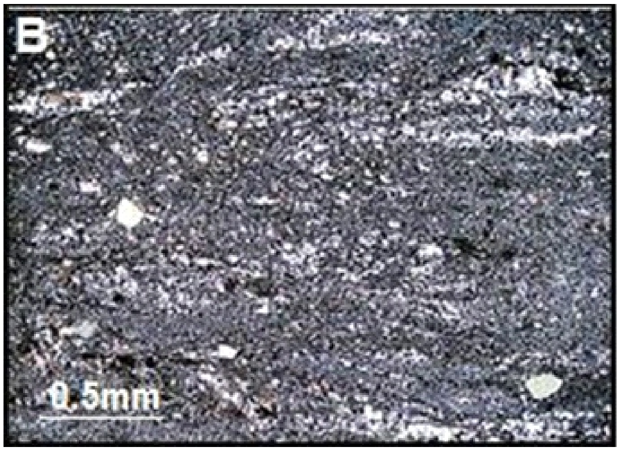

Fig. 14-A & B: Ignimbrite with noticeable flow of fragments.

5 – Geochemical Analyses

Chemical Rating and Nomenclature: Results of chemical analyses of the studied samples are illustrated in Table (1). In chemical diagram of SiO_2 versus $Na_2O + K_2O$, rocks of Hassan Abad Region are classified in rhyolite interval (Diagram 1).

Taking into account the fact that cations have a more favorable distribution with respect to weight percentage of the oxides and better reflect the rock composition, classification diagram of De La Roche *et al.* (1980) can be used for nomenclature of the rocks. Involvement of chemical composition of all principle elements of the rock in the respective classification and application of this diagram for all igneous rocks are among the benefits of using the respective diagram (Rollinson, 1993). In this diagram, parameters R_1 and R_2 is defined as below:

$R_1 = 4\,Si - 11(Na + K) - 2\,(Fe + Ti)$

$R_2 = 6\,Ca + 2\,Mg + Al$

The respective rocks lie within the rhyolite interval (Diagram 2).

In addition, based on ratio of Zr/TiO_2 to SiO_2, the analyzed samples in this diagram are placed within rhyolite and riodacite area (Diagram 3). In another diagram plotted based on ratio of Nb/Y to Zr/TiO_2, the region lies in the trachy andesite and riodacite extent (Diagram 4).

In SiO_2 versus $Na_2O + K_2O$ diagram, the studied rocks are classified in sub-alkaline interval, and, they lie in calc-alkaline magma series based on AFM diagram (Diagrams 5 & 6). Variations of $Al_2O_3/(CaO + Na_2O + K_2O)$ versus $Al_2O_3/(Na_2O + K_2O)$ magmas indicates alumina (aluminum oxide) based on saturation degree. In the respective diagram, the analyzed samples are classified as peraluminous rocks that might imply contamination with crustal materials (Diagram 7).

Nb/Y versus Rb/Y diagram was used for elemental enrichment of analyzed rocks in association with tectonic environments. In the respective diagram, the samples nearly lie above Rb/Nb = 1, indicative of enriched intra-plate environments, enriched subduction zone and/or crustal pollution (Diagram 8).

In Rb/Zr versus K_2O/Na_2O diagram, the studied samples are classified in AFC series that can demonstrate occurrence of partial crystallization and impact of contamination processes in the region's volcanic rocks (Diagram 9). The studied samples lie in magmatic contamination and mixing interval according to K_2O versus MgO diagram (Diagram 10). To determine tectonic position of the region's rocks based on Zr versus Y diagram, the results show that the analyzed rocks have been formed in arc-dependent tectonic setting (Diagram 11).

According to Al_2O_3 versus TiO_2 diagram, volcanic rocks of the region lie in the magmatic arc-dependent tectonic environment (Diagram 12). This diagram divides the magmatic arc tectonic environment into two environments of oceanic volcanic arc and continental volcanic arc.

According to Diagram 13, the analyzed samples were classified in the active continental volcanic arc zone.

The studied samples have been normalized to chondrite and enrichment of LREEs (light rare earth elements) compared to HREEs ((light rare earth elements)) can be observed. LREEs were more incomptaible than HREEs. Slight difference of ion sizes leads to relative greater incompatibility of LREES compared to HREEs. Therefore, LREEs have larger concentration in the residual fluid in comparison with heavy metals. Another reason for enrichment of LREEs is their high mobility as a function of fluid behavior (Rollinson, 1993). Since the respective elements were concentrated in continental crust, their concentration in magma could suggest contamination with crustal substances. Amounts and abundance of rare earth elements (REEs) in Hassan Abad rocks normalized to chondrite exhibit a relatively regular pattern and greater enrichment is observed in LREE elements compared to HREE counterparts (Diagram 14).

Also, based on spider diagram normalized to crustal average (Diagram 15), all samples exhibite negative Nb and Ti anamolies, which is in alignment with linkage of the samples with subduction and orogenic zone. K, Rb, and Th enrichment is observed in the samples as well, which is a characteristic of crustal rocks. Indeed, negative Nb anamoly is characteristic of continental rocks and represents crust involvement in magmatic processes.

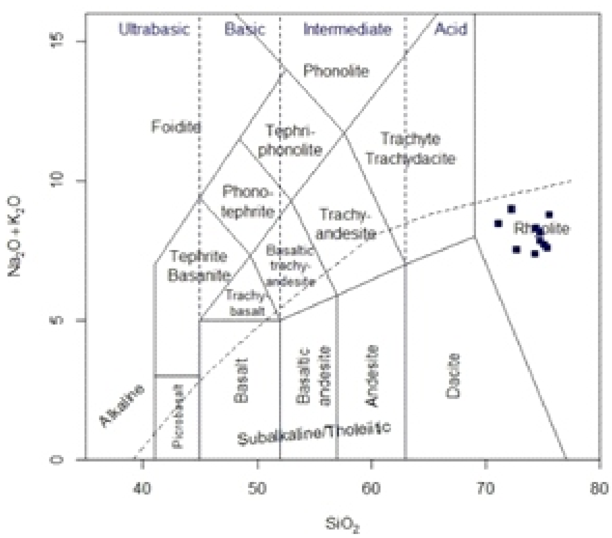

Diagram 1– Position of samples in SiO_2 versus $Na_2O + K_2O$ diagram

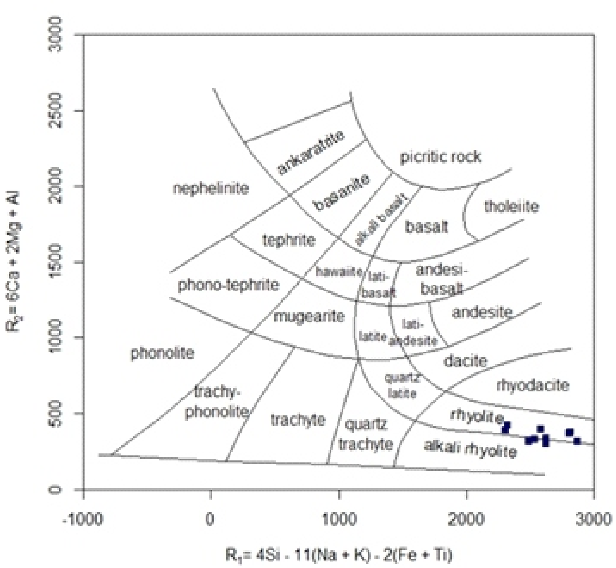

Diagram 2 – Position of the analyzed rocks in SiO_2 versus R_1 and R_2 diagram

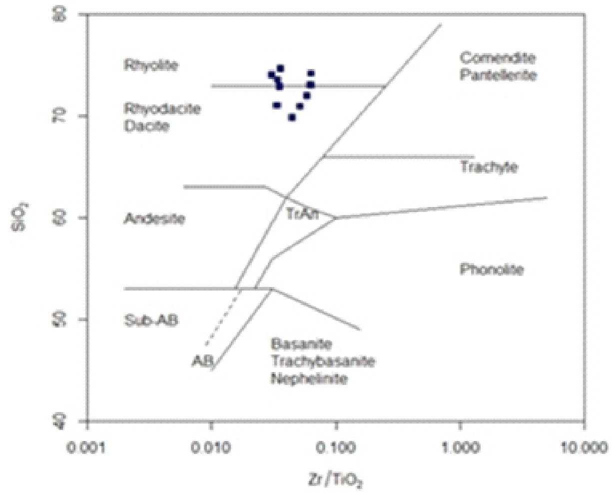

Diagram 3 - Position of the analyzed rocks in SiO_2 versus Zr / TiO_2 diagram

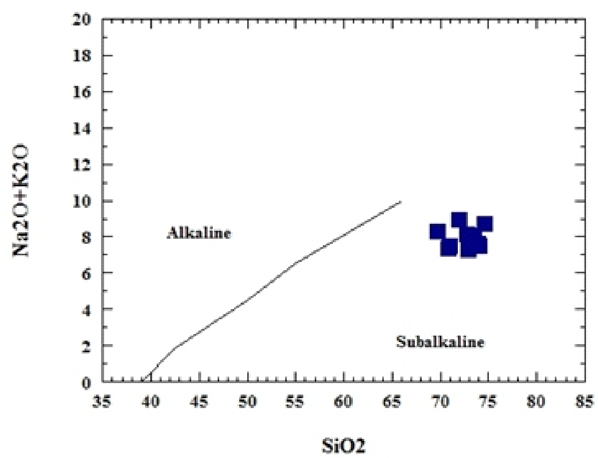

Diagram 4 – Nomenclature of rocks based on Nb/Y versus Zr / TiO_2 diagram

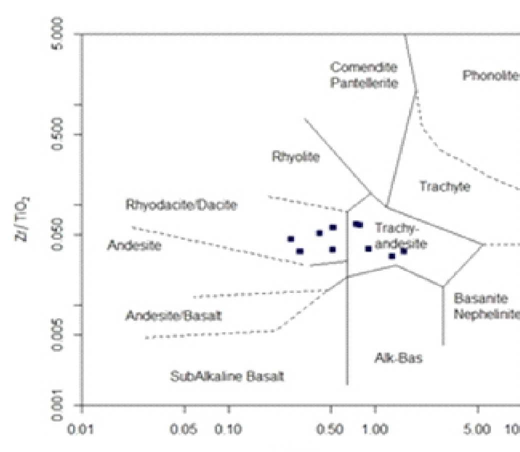

Diagram 5– The studied samples are positioned in sub-alkaline interval

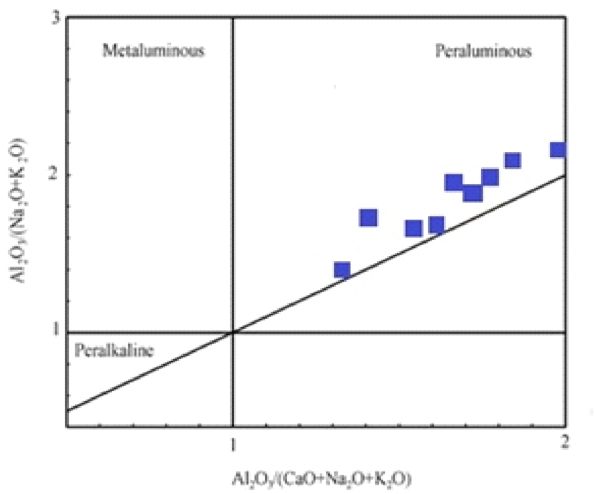

Diagram 6 – Magmatic series of all samples is calc-alkaline

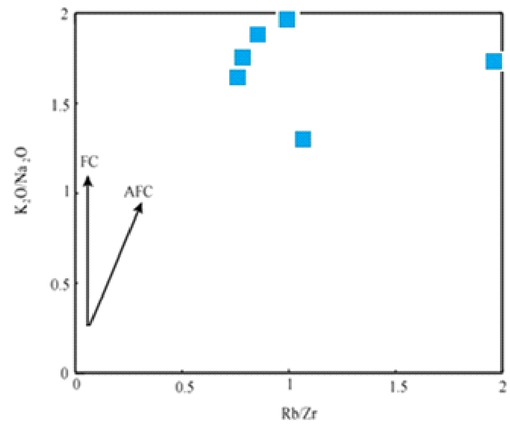

Diagram 9 – Position of sample in AFC interval indicates occurrence of partial crystallization and impact of contamination processes in volcanic rocks of the region

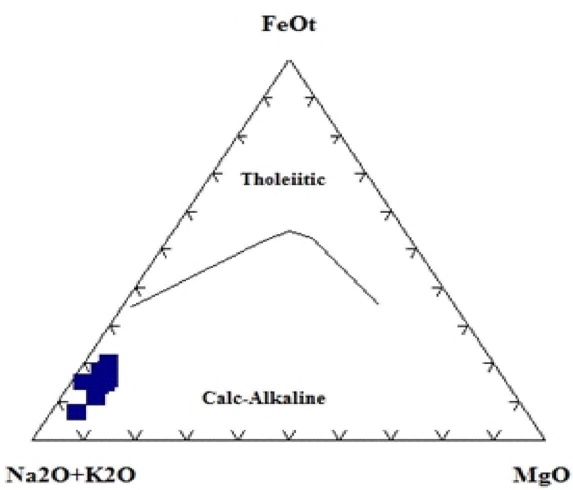

Diagram 7 – The samples lie in peraluminous zone

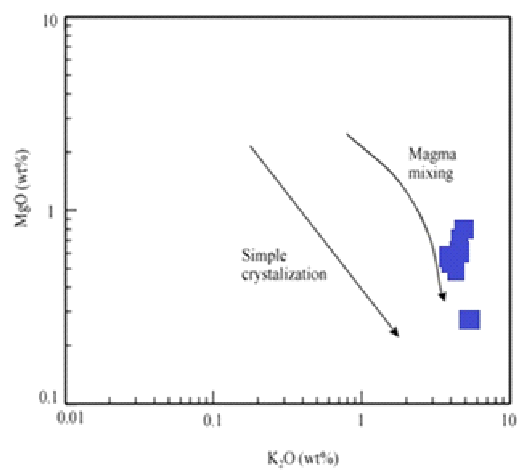

Diagram 10 – Position of samples in magmatic contamination and mixing zone

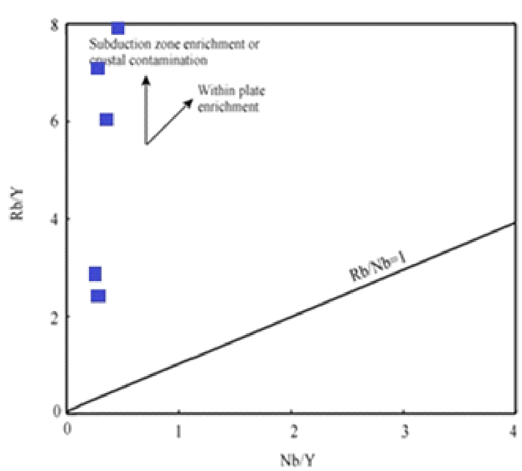

Diagram 8 – The studied samples have a trend of enriched subduction zone or crustal contamination

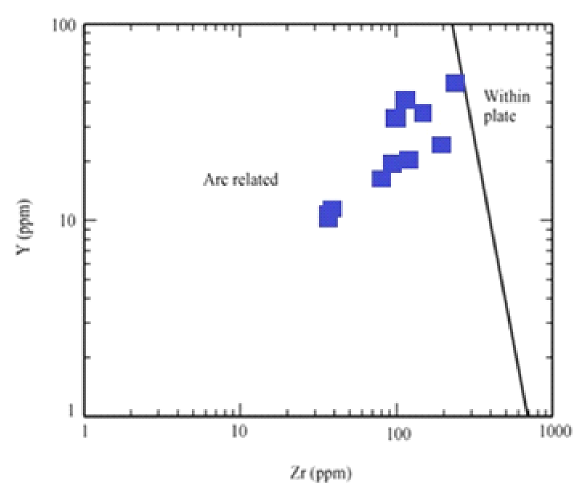

Diagram 11 – The analyzed samples have been formed in an arc-dependent tectonic environment

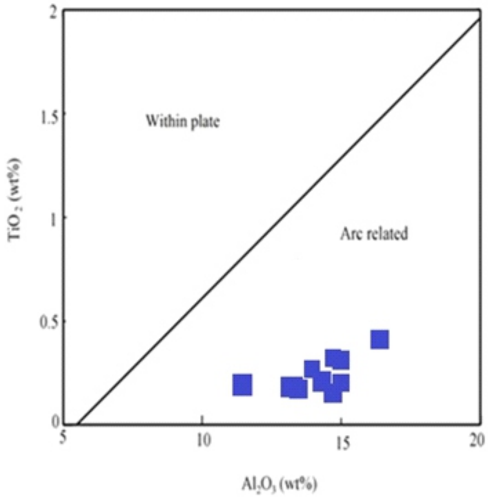

Diagram 12 – Position of samples in magmatic arc-dependent environments

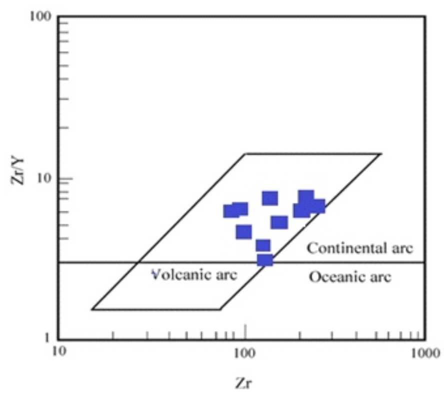

Diagram 13 – Zr versus Zr/Y diagram indicate continental volcanic arc environment for the region's rocks

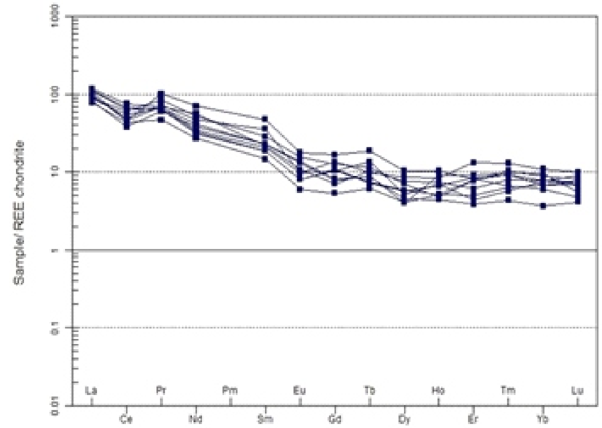

Diagram 14 – REE pattern nromalized to chondrites

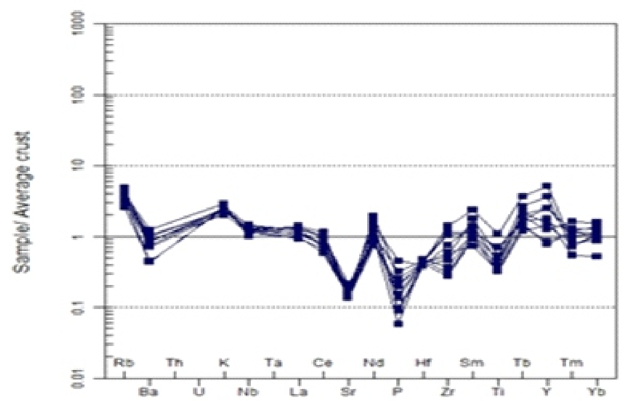

Diagram 15 –Values of rare elements of Hassan Abad normalized to crustal average

Conclusion

Morphologically Hassan Abad Region is situated as low-elevation individual to interconnected hills along the great fault of Qom – Zofreh with a northern – southern trend. The rhyolites consist of quartz, plagioclase, alkali feldspar minerals and glass fragments. The tuffs are of crystaline, vitric and ignimbrite in which no differentiable stucture is detected (such as bedding or textural facies change). In addition, in terms of texture, pyroclastic, cryptocrystaline, and sphereolitic rocks are observed. According to geochemical studies and diagrams, the constituent magma of the respective rocks with rholitic composition is classified in calc-alkaline series which is also indicative of peraluminous composition for the region's rocks. Furthermore, the plotted spider diagrams normalized to chondrite and upper crust revealed that the samples of the studied region have originated from partial melting of crustal rocks. The studied pyroclastic rocks have outrcrop along the strike-slip Qom Zofreh fault. Also, discordant trends of Uremia – Dokhtar Belt and reverse faults as well as regional dykes according to Rieldel model imply that most volcanic and volcanoclastic rocks have been emplaced under simple shear stress in the shear – compressional system (Bargowhar and Marbin – Rangan faults and Kachumesghal – Ganyan fault), and, Cenozoic intrusive – volcanic sequences of this region result from faulting of subductive plate during the stage following continental collision. Ultimately, according to the conducted geochemical studies and emplacement of ignimbrite in the extensional spaces created in the region is not similar to rifting or intracontinental rifts but the respective rocks have been emplaced in a extensional – faulting system having the same trend as the major regional structures. Consequently, the hypothesis of subduction of young Tethys Ocean beneath Central Iran Subzone is onfirmed according to findings of the present research.

Table 1– Analysis results of Hassan Abad Region

Sample No	H-2	H-3	H-6	H-9	H-42	H-45	H-23	H-37	H-16	H-19
SiO_2	74.15	74.65	71.98	69.82	72.02	74.03	73.05	73.53	72.87	70.96
TiO_2	0.196	0.215	0.409	0.548	0.193	0.191	0.251	0.32	0.28	0.423
Al_2O_3	14.33	12.68	15.32	16.59	13.48	15.15	15.28	14.05	13.82	15.81
Fe_2O_3	1.55	1.78	1.36	1.93	2.24	0.68	1.46	1.58	2.06	1.97
MnO	0.038	0.019	0.018	0.01	0.022	0.024	0.012	0.021	0.017	0.019
MgO	0.67	0.26	0.76	0.77	0.49	0.46	0.52	0.61	0.47	0.53
CaO	0.33	0.54	0.78	0.22	0.15	0.46	0.49	0.26	0.34	0.56
Na_2O	2.31	3.36	2.83	2.83	2.54	2.76	2.62	2.92	3.02	3.08
K_2O	5.15	5.31	6.09	5.45	4.89	4.82	4.63	5.08	5.09	4.24
P_2O5	0.04	0.011	0.064	0.047	0.037	0.026	0.086	0.018	0.017	0.029
LOI	1.18	1.13	1.19	1.37	1.64	1.53	1.5	1.26	1.49	1.48
Total	99.944	99.955	100.801	99.585	97.702	100.131	99.899	99.649	99.474	99.101
Rb	158	220	242	217	235	227	295	195	209	254
Sr	69	77.6	72.8	72.3	72.6	105.8	89.6	98.5	76.9	76.2
Zn	21	56	65	15	33	12	43	39	51	35
Ba	313	588	873	307	740	600	498	529	704	624
Co	2	3	4	2	2.5	2.4	3.8	2.9	3.1	2
Ta	1.35	1.4	1.5	0.5	1.66	0.71	1.29	1.06	1.28	0.96
Cs	5.9	4.9	5.3	6.8	7.3	5.7	6.2	5.8	7.1	5.6
Hf	1.98	2.25	2.13	2.08	2.12	1.95	1.86	1.94	1.79	2.07
Nb	15	15.9	13	19	17.2	15.3	16.9	15.6	18.1	14.9
Ni	10	1	10	16	1	2	7	15	12	9
Zr	124	77	240	292	65	58	157	109	98	218
Y	20	17.6	25	71	10.8	11.7	21.5	50.5	35.2	35.4
La	25.9	39	27.4	32.7	37	36	29.8	31.2	35.4	28.6
Ce	38	65	33	40.1	58	56	53	42.5	39.8	48
Pr	5.23	7.68	6.75	11.3	7.13	7.31	9.56	8.26	7.68	7.58
Nd	17.2	21.7	24	44.3	19.4	20.6	32.6	29.8	35.9	26.3
Sm	2.99	4.24	4.7	9.67	3.8	3.81	5.84	7.24	4.37	4.59
Eu	0.46	0.75	1.06	1.36	0.62	0.62	1.19	0.75	0.83	1.01
Gd	1.47	3.74	2.26	4.62	2.95	2.99	3.48	2.87	1.94	2.15
Tb	0.29	0.46	0.4	0.88	0.34	0.35	0.53	0.64	0.49	0.41
Dy	1.4	2.97	1.56	3.54	1.98	2	2.42	1.76	2.59	1.38
Ho	0.36	0.58	0.31	0.72	0.46	0.36	0.33	0.49	0.51	0.64
Er	1.14	2.99	0.87	1.86	1.9	1.8	1.75	0.98	1.37	2.06
Tm	0.19	0.39	0.13	0.2	0.28	0.28	0.31	0.17	0.24	0.29
Yb	1.5	2.4	0.8	1.32	1.7	1.5	1.95	1.68	1.69	2.09
Lu	0.26	0.34	0.14	0.16	0.26	0.23	0.28	0.31	0.24	0.19

References

Emami M. and Houradfar J. (2010): 1:100,000 Geological Map of Ardestan, Tehran, "Iran Geological Survey and Mining Explorations Organization"

Emami M. H. (2000): Magmatism in Iran, Tehran, "Iran Geological Survey and Mining Explorations Organization", 18, 622.

Pourmansouri M. (2015): Petrological Analysis of Neogenic Pyroclastic Masses of Rangan – Shourghestan (South Ardestan – Northeast Esfahan) with an Emphasis on Dependent Alterations; Master Thesis of Payam-e Nour University of Shahin Shahr, 93.

Mohjal M. (2000): Role of Extensional Spaces in Activity of Igneous Rocks in Kashan – Ardestan Region; A Model for Formation of Uremia – Dokhtar Volcanic Arc, Tehran, 19th Conference of Geoscience, "Iran Geological Survey and Mining Explorations Organization".

De La Roche H. Leterrier J. Grande Claude P. and Marchal M. (1980): A classification of Volcanic and plutonic rocks using R_1-R_2 diagrams and major element analyses– its relationships with current nomenclature, chemical. Geology, 29, 183-210.

Fisher R. V. and Schmincke H. V. (1984): Pyroclastic rocks, Springer, Heidelberg, 472.

Fisher R. V. (1966): "Mechanism of deposition from pyroclastic flows." American Journal of Science, 264.5 350-363.

Rollinson H. R. (1993): Using geochemical data, Evaluation, Presentation, Interpretation: Wesley Longman, Harlow.

Sylvester A. G. (1988): Strike-slip faults. Geological Society of America Bulletin 100:1666–1703.